The Visual Computer
https://doi.org/10.1007/s00371-021-02154-x

ORIGINAL ARTICLE

Degenerative disc disease diagnosis from lumbar MR images using hybrid features

A. Beulah[1] · T. Sree Sharmila[2] · V. K. Pramod[3]

Accepted: 27 April 2021

Abstract
Disc degeneration is a common type of lumbar disc disease. Disc degeneration leads to low back pain, and it is caused due to injury in Intervertebral Disc (IVD). An automatic diagnostic system to diagnose degenerative discs from T2-weighted sagittal MR image is proposed. A fully automated Expectation-Maximization (EM)-based new IVD segmentation is proposed to segment the lumbar IVD from mid-sagittal MR image. Then, a hybrid of basic intensity, invariant moments, Gabor features are extracted from segmented IVDs. The IVDs are classified as degenerative or non-degenerative using Support Vector Machine (SVM) classifier. The proposed system is trained, tested and evaluated for 93 clinical sagittal MR images of 93 patients. The optimized hyperparameters are estimated. The proposed model is tested and validated for the dataset and obtained an accuracy of 92.47%. The patient-based analysis was performed and obtained an accuracy of 92.86%. The performance analysis of the proposed model with other classifiers like k-NN, decision tree, Linear Discriminant Analysis (LDA) and Feedforward neural network is also analyzed. This proposed method outperforms when compared with state-of-the-art methods. This system can be used as a second opinion in diagnosing degenerative discs.

Keywords Disc degeneration · Expectation-Maximization · Gabor features · Invariant moments · Low back pain · Lumbar spine · Magnetic Resonance Imaging · Support Vector Machine

1 Introduction

In human, low back pain is the most common life-long disability [1]. Global Burden of Disease (GBD) reports showing that in 2015, the 4^{th} leading cause of Disability-Adjusted Life Years (DALYs) globally is low back and neck pain [2]. The study reports low back and neck pain was positioned 12^{th} in 1990 and 8^{th} in 2005. Over a span of 10 years, the impact associated with the same rose drastically for the age group of 25 to 64 all over the world. This shows a lack of attention, resources and research about this condition.

The primary cause of low back pain is mainly due to strain and stress given to the lumbar spine [3]. Any injury that occurs in the spinal column affects a person's mobility ranging from lower back pain to paralysis. The common types of lumbar spine injuries are disc degeneration, bulge, herniation, spinal canal stenosis, etc. The first step in analyzing the cause for pain is a subjective physical examination and is based on the signs and symptoms to find the involvement of neurological conditions [4]. After ruling out non-neurological cases, for further analysis of the injury and if the pain is progressive, physicians recommend an imaging study of the lumbar spine region [5].

The human spinal column provides central support to different organs and provides flexibility to the body. The lumbar spine consists of 5 vertebrae (L1 to L5) and 6 Intervertebral Discs (IVDs) (T12-L1 to L5-S1). The annulus fibrosus and nucleus pulposus form an IVD. The annulus fibrosus is composed of fibers, and nucleus pulposus is a gel-like struc-

✉ A. Beulah
beulaharul@ssn.edu.in

T. Sree Sharmila
sreesharmilat@ssn.edu.in

V. K. Pramod
pvalsalam@gmail.com

1 Dept. of Computer Science and Engineering, Sri Sivasubramaniya Nadar College of Engineering, Chennai, India

2 Dept. of Information Technology, Sri Sivasubramaniya Nadar College of Engineering, Chennai, India

3 Dept. of Orthopaedics, Trivandrum Medical College, Thiruvananthapuram, India

Published online: 08 May 2021

ture with 70% of water content. The IVD acts like a shock observer and separates vertebrae. IVDs help the body to be flexible and prevents vertebrae from rubbing against each other due to stress and strain occurring in the body. Degeneration often happens due to ageing, trauma or accident. Disc degeneration is dehydration of water content in the nucleus pulposus, causing the disc to be short, inflexible and vulnerable to tear the annulus fibrosus. When one IVD dehydrates, it can change the mechanics, structure of the lumbar spine especially the region surrounding IVD.

Various medical imaging modalities such as X-ray, Ultrasound, Computed Tomography (CT), Magnetic Resonance Imaging (MRI), Positron Emission Tomography (PET) exist. These modalities have remarkably improved the process of diagnosis in numerous diseases. MRI does not require any radiations or radioactivity, and hence, there are no harmful side effects. The soft tissues like IVDs, spinal cord are precisely visible in MR image than in either CT or X-ray [6].

There are different protocols of MR images, among which T1 and T2-weighted are most popular. Here, the different tissues are characterized by the relaxation times T1 and T2. In T1-weighted MR images, there is no much difference in the intensity ranges for soft tissues, spinal cord and IVDs. Whereas, in T2-weighted images, the soft tissues with and without disease, spinal cord, vertebrae have different intensity ranges [7]. In a T2-weighted image, a decrease in IVD intensity denotes dehydration, which means reduction in hydrogen ions. Therefore, a low signal intensity for an IVD in T2-weighted image is a disc degeneration [8]. Figure 1 shows normal and degenerated IVDs. The lumbar discs L1-L2, L2-L3 and L3-L4 are marked as normal and L4-L5 as degenerative disc. The degenerative discs are diagnosed from the mid-sagittal lumbar MR image.

A Computer Aided Diagnosis (CAD) system will assist the radiologist to ease their burden in the analysis of medical images. CAD serves as a second opinion for the radiologist [9]. In recent research, an automatic CAD system to segment IVD and diagnose disc degeneration was done based on sagittal MR images. Few limitations are identified from the existing system. To overcome the limitations, an Expectation-Maximization (EM)-based new IVD segmentation is proposed to segment the IVDs. Also, a Support Vector Machine (SVM)-based classification is proposed to classify each IVD as degenerative and non-degenerative. All programs related to IVD segmentation and disc degeneration diagnosis are implemented in MATLAB 8.6. Experiments were run on a computer with an Intel i5 processor running at 2.30 GHz using 8 GB of RAM.

The rest of this paper is organized as follows: Section 2 describes the related work. Section 3 discusses the proposed architecture to diagnose degenerative discs from mid-sagittal MR images. The experimental results and the discussions are explained in section 4. Finally, the paper concludes in section 5.

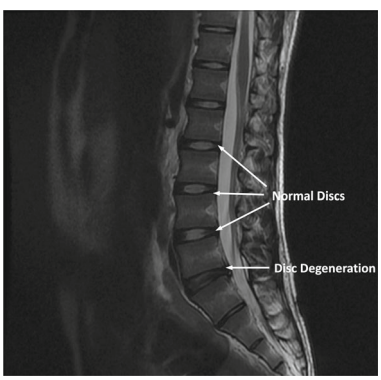

Fig. 1 Mid-sagittal lumbar MR image showing degenerative and non-degenerative discs

2 Related Work

In this section, the research issues related to IVD segmentation and degenerative disc diagnosis are discussed. Segmenting the IVD is a fundamental step to analyze each IVD for any abnormality. In the literature, several methods were proposed to segment the lumbar spine structures [10–15]. Similarly, various methods were suggested to diagnose disc degeneration [16–22]. A summary of different IVD segmentation and degenerative diagnosis methods is tabulated in Table 1.

From Table 1, it is noted that most of the degenerative disc disease diagnosis was designed using machine learning techniques. Few limitations are identified from the existing system. If an abnormality is present in a disc, few approaches failed to segment the IVD effectively. In the segmentation method proposed by Ayed et al. [10], a reference object prior needs to be mentioned in the image. Another segmentation method [11] fails to segment an abnormal disc. Unal et al. [23] extracted the features from axial slices manually. Castro et al. [22] extract eight different features from manually segmented IVDs. In certain conditions, the height of degenerative discs is similar to that of healthy discs (minor abnormality). The method developed by Mahdy et al. [16] could not identify such degenerative discs.

To overcome these limitations, in this paper, a new approach to diagnose degenerative discs from T2-weighted mid-sagittal MR image is proposed. The sagittal MR image consists of vertebrae, sacrum, coccyx, spinal cord, IVDs of thoracic and lumbar spine. In this work, lumbar IVDs only are selected for the diagnosis process. In general, decrease in hydration leads to disc degeneration. Therefore, the pixel intensity values are much lesser than normal discs. Moreover, the height of thoracic IVDs is usually smaller than

Table 1 Summary of IVD segmentation and Degenerative disc diagnosis

S. no.	Method	Dataset	Inference
1.	Graph Cuts with Invariant Object Interaction to segment the IVD Priors [10]	10 T2-weighted mid sagittal lumbar MR images	Acquires information about the geometric interactions between various objects within the image. A reference object needs to be mentioned in the image
2.	ML-based method to diagnose lumbar disc disease [11]	T2-weighted sagittal images for 30 subjects	IVDs were labelled by fitting a third-order polynomial. Could not segment abnormal disc, if the disc is degenerative
3.	Desiccation diagnosis using probabilistic model [17]	T2-weighted MR Images for 55 subjects	Gibbs distribution to extract features. Handles the relation between IVDs at object level
4.	Comparison of feature extraction techniques for diagnosis of lumbar degenerative disc disease [19]	45 saggital MR images for 9 subjects	Gray-Level Co-Occurrence Matrix (GLCM) and Average Absolute Deviation (AAD) features were extracted. The discs were classified by Multilayer Perceptron - Artificial Neural Network (MLP-ANN)
5.	Automatic diagnosis of degenerative disc disease using ANN [20]	60 saggital MR images for 12 subjects	Wavelet transform to extract the features. The discs were classified by MLP-ANN
6.	3D morphological and intensity features for detection of IVD degeneration [21]	First set consists of MR images for 28 subjects, second set for 16 subjects	Morphological, appearance features were extracted. Classification using Linear Discriminant Analysis (LDA) and SVM
7.	CAD system to diagnose degenerative discs [13]	T1, T2 -weighted mid-sagittal MR images for 102 subjects	Segmentation using AAM and classification using SVM. Reference objects needs to be mentioned
8.	Semiautomatic diagnosis of degenerative discs [18]	T2 weighted MR images for 42 subjects	Texture features were extracted. Classification using ANN. Overfitting during training
9.	IVD classification by its degree of degeneration [22]	T2 weighted MR images for 48 subjects	Intensity features were extracted. Classification using ANN. Manual selection of IVD center
10.	Automatic detection system for degenerative disc [16]	Sagittal, Frontal, and Axial view of CT images for 10 cases	Segment the vertebra. Find the distance between the adjacent vertebra. Does not diagnose degenerative discs if the height of degenerative disc is similar to that of normal disc

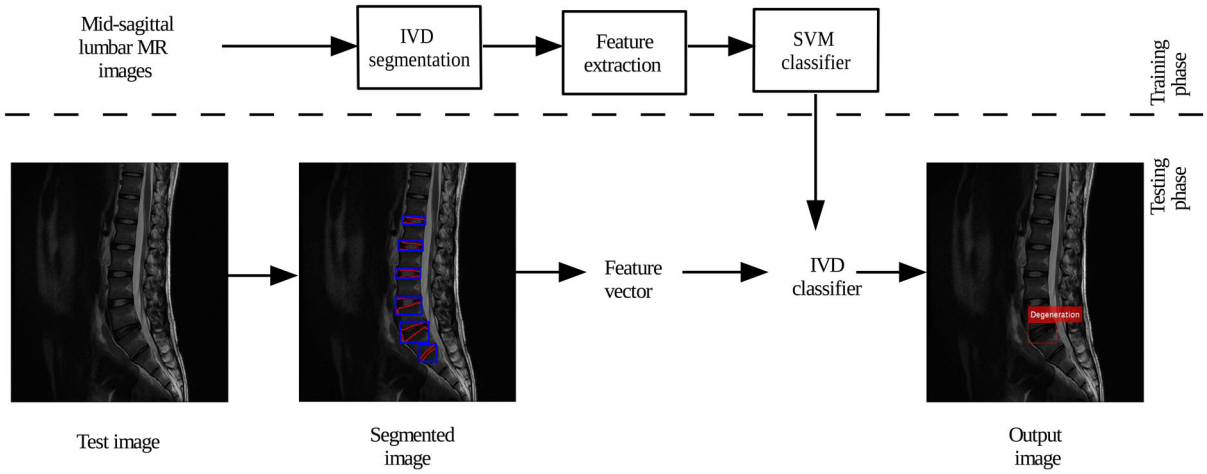

Fig. 2 Architecture of degenerative disc disease diagnostic system

lumbar IVDs. If an IVD is degenerated and herniated, the height becomes smaller and this size may match with the size of normal thoracic IVD which leads to an inconsistent diagnosis. Hence, it is easy to select the lumbar IVD from the segmented image. A reduced level in the IVD intensities represents the degeneration. In degeneration, the signal intensity plays a major role. Also, it is identified that intensity-based features are perfect. Hence, a new IVD segmentation method to segment the lumbar IVDs and a hybrid feature set are proposed.

3 Degenerative disc disease diagnostic system

The proposed system to diagnose the degenerative disc is shown in Fig 2. The mid-sagittal lumbar MR image is the input to this system which contains lumbar spine and its surrounding organs. Hence, it is necessary to segment the lumbar IVDs from MR image. The new segmentation algorithm segments the needed lumbar IVDs. A tight bounding box is generated over the segmented region in the original image. The degenerative and non-degenerative discs are separated to form the dataset, with the help of a medical expert. Then, the hybrid features are extracted for IVD regions. The model is built by trained features using SVM. When a new test image is given to the model, the image is automatically segmented to obtain lumbar IVDs and classifies each lumbar IVD as either disc degeneration or non-degeneration.

3.1 Intervertebral disc segmentation

The mid-sagittal MR image consists of all lumbar IVDs, a few thoracic IVDs, corresponding vertebrae, spinal cord and other organs surrounding the spinal column. The lumbar IVDs alone are necessary to diagnose the disease.

The automatic EM- and morphology-based segmentation proposed in our previous work [14] could only segment a single IVD present in the axial image as a single connected component, whereas in sagittal images more than one IVD is present which are not segmented. Moreover, the morphological open removes all small components present in the axial image, which could remove degenerated IVDs in the sagittal image. Hence, for these reasons, EM and morphology-based segmentation algorithm could not segment IVDs present in mid-sagittal MR image. Therefore, a new fully automatic segmentation to segment IVD from mid-sagittal MR image is proposed.

The algorithm to segment lumbar IVDs is presented in Algorithm 1. First, EM segmentation algorithm [24] is applied to the mid-sagittal image I. This produces the EM segmented image I_{EM}. The regional maxima for I_{EM} is found and referred to as I_{RM}. The regional maxima is used to identify local peaks in an image. This step highlights the spinal column region. The obtained I_{RM} is a binary image. This binary image is complemented, and morphological operators like filling holes, thinning and opening are performed to generate I_M. The complementation highlights the IVDs in images. The complementation and morphological operators are necessary to separate the IVDs and to get proper IVD region.

The logical operator is applied on I_M to eliminate unwanted components in it. This produces image I_L. Even now, few unwanted components are left out. Then, the tilt angle θ for each component in I_L is found. A connected component is removed from I_L, if θ is beyond the tilt angle threshold θ_t, to obtain the segmented image S. The obtained image S consists of all lumbar and a few thoracic IVDs.

Algorithm 1: Algorithm to segment lumbar IVDs from mid-sagittal lumbar MR image

Input: Mid-Sagittal lumbar MR image I
Output: Segmented image S

1. Find the EM segmented image I_{EM}.
2. From I_{EM}, find the regional maxima and refer it as I_{RM}.
3. Complement the image I_{RM} to obtain I_C
4. In I_C perform holes filling, thinning and opening to obtain I_M.
5. Remove the unwanted components from I_M using logical operators. The image obtained is referred as I_L.
6. For each connected component in I_L
   (a) Find the tilt angle θ.
   (b) If θ beyond θ_t, then remove the component from I_L to get a new image S.

return *S the segmented image*;

Select the lower six IVDs as lumbar IVDs. This automatic segmentation procedure is shown in Fig 3.

3.1.1 Regional maxima

An image can have more than one regional maxima or minima, but it can have only one global maxima and minima. In a grayscale image I, the regional maxima is a connected component of pixels with a constant height h such that each pixel in the neighbourhood of the maxima has pixel value strictly lower than h [25]. The pixels for the regional maxima are assigned as ones and all other pixels as zeros. Hence, the image I_{RM} obtained is a binary image.

3.1.2 Morphological operations

In I_{RM}, degenerated discs contain zero pixel value, while other discs consist of one pixel value because they contain water in them. In order to obtain all IVDs as white on a dark background, it is required to complement I_{RM}, and further applying morphological operators on the complemented image. The complemented image is represented as I_C. In image I_C, there are holes in IVD. A hole is defined as a background region surrounded by a connected border of foreground pixels [26]. The holes are filled using morphological hole filling. Morphological thinning and open [26] are used to remove the connectivity between IVDs.

3.1.3 Logical XOR operator

The IVD needs to be extracted from image I_{open}. Hence, after finding morphological open, a lower and upper bound

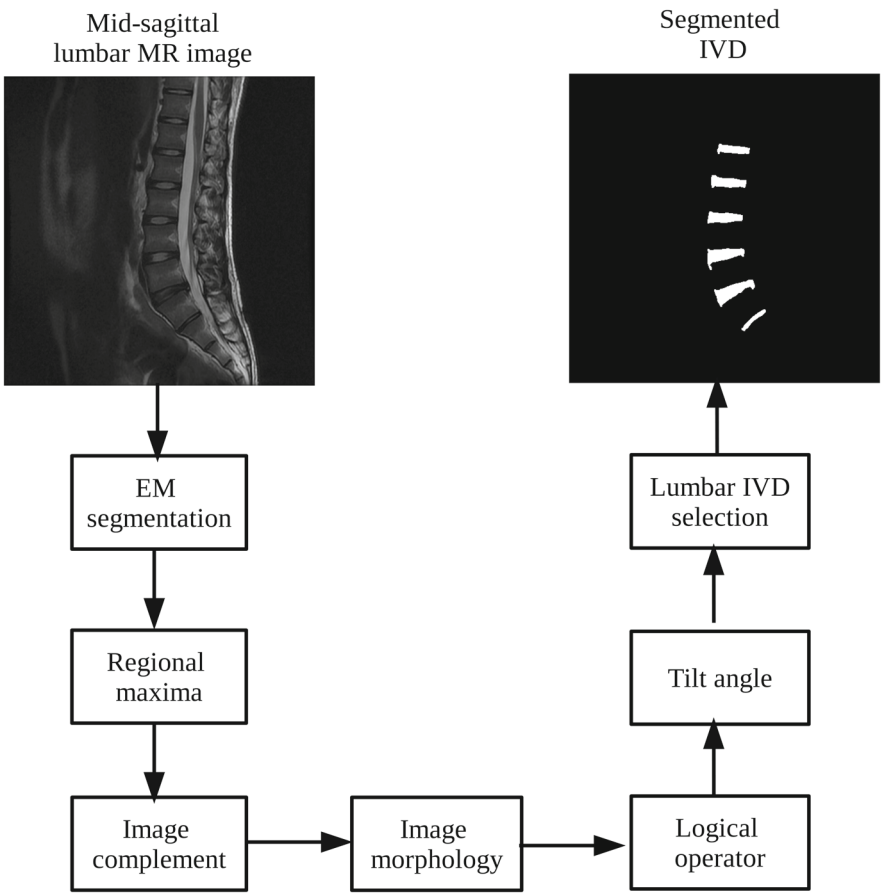

Fig. 3 Architecture of the IVD segmentation from mid-sagittal MR image

(a) After complement (b) After holes fill (c) After thin (d) After open

Fig. 4 The image morphology process in MR image (sample region is shown)

is fixed. A binary image L is obtained with the size of components less than the lower bound. Another binary image U is obtained with the size of components greater than the upper bound. The logical XOR operation is performed on these two images (L, U) to obtain the desired output, i.e. the image I_L. I_L consists of segmented IVDs and neighbouring components.

3.1.4 Tilt angle

After applying morphological and logical operators, the tilt angle θ for each component in I_L is found. The tilt angle θ for a component is the angle between the baseline and the line through the major axis of that component. The tilt angle for a component is shown in Fig 5. Generally, the tilt angle of an IVD lies between -10.5 ± 4.5 (mean $\pm$ standard deviation) and 35.6 ± 10.2 [27]. The reason being the IVD lies between the specified tilt angle threshold θ_t, if a component's θ is beyond θ_t, then the component is not an IVD. Such components are removed from the image I_L. This step is used to distinguish the IVDs from other components in the image. Overall, the proposed segmentation method does not need any object reference and segments all lumbar IVDs, even though it has abnormalities.

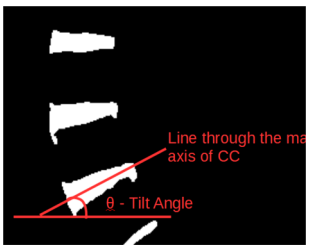

Fig. 5 Tilt Angle of a Connected Component

3.1.5 Lumbar IVD extraction

The lumbar IVD alone is extracted from the segmented image S. A lumbar sagittal MR image usually consists of full lumbar spine and lower part of the thoracic spine. This image approximately has 9 IVDs (6 lumbar IVDs and remaining thoracic IVDs). This number varies for individuals. The center point for each IVD in S is found. The center points found are in random order. The center points of IVDs are sorted in ascending order with respect to X-axis, so that, lower six IVDs are identified. Now, these lower six points are center points for the lumbar IVDs. The remaining points are center points of thoracic IVDs and are left out. In this method, sacralization and lumbarization are not considered. The IVD segmentation for a sample MR images is shown in Fig 6.

The boundary for all lumbar IVDs is extracted. The boundary for each IVD in the segmented image S is denoted by $\beta(ivd_b)$ [26]. $\beta(ivd_b)$ is defined as:

$$\beta(ivd_b) = S - (S \ominus sel) \tag{1}$$

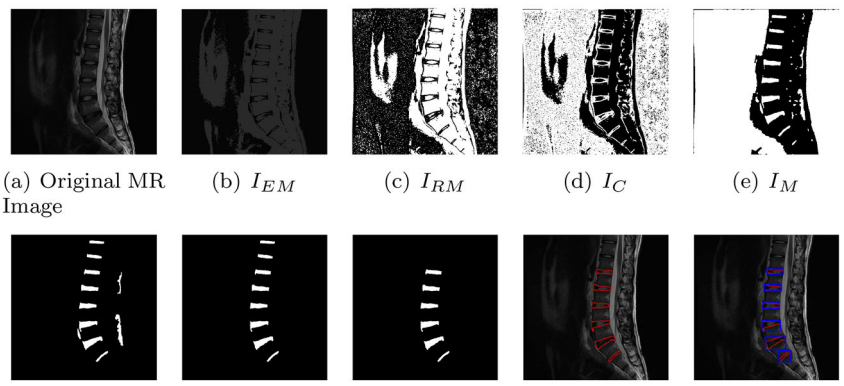

(a) Original MR Image (b) I_{EM} (c) I_{RM} (d) I_C (e) I_M

(f) I_L (g) Tilt Angle S (h) Lumbar IVD (i) Lumbar Boundary (j) Bounding Box

Fig. 6 The EM-based new IVD segmentation process for an MR image

where sel is SE, $S \ominus sel$ is the erosion of S by sel. This boundary is marked in the mid-sagittal MR image. A tight bounding box is marked over the boundary. This bounding box region is cropped from the grayscale image of mid-sagittal MR image as a lumbar IVD (ivd). The bounding box is obtained from the major and minor axis of an IVD. The lumbar IVDs are partitioned as degenerative disc (ivd_D) and non-degenerative disc (ivd_{ND}) with the help of a medical expert.

3.2 Feature extraction

After cropping and separating the desired lumbar IVDs as degeneration (ivd_D) and non-degeneration (ivd_{ND}), features are obtained from them. Here, there is a drastic variation in the intensity values between degenerative and non-degenerative discs. The IVDs varied in size and arranged in different angles to form lumbar curve lordotic. As the disc loses its water content, the texture also varies between the discs. The Gabor features are invariant to rotational and scaling which is the main advantage over other texture features. Hence, a hybrid of basic intensity, moments and Gabor features are extracted from the IVDs. The extracted features are explained in the following sections.

3.2.1 Basic intensity features

The basic intensity features such as maximum, minimum, mean intensity values, length of the major and minor axis, eccentricity and intensity histogram are extracted for each IVD (ivd). The maximum, minimum and mean intensity values for an image ivd are denoted by $max(ivd)$, $min(ivd)$ and $\mu(ivd)$, respectively.

The points of the major axis (x_i, y_i) and (x_j, y_j) are obtained from the diameter of boundary $\beta(ivd_b)$. The diameter is calculated as [26]:

$$diameter_{\beta(ivd_b)} = \max_{i,j} \left[D(\,(x_i, y_i),\ (x_j, y_j)\,) \right] \tag{2}$$

where D is the distance measure. The minor axis is the longest line perpendicular to the major axis. The major and minor axis marked for two different IVDs are shown in Fig. 7.

The intensity histogram [26] of image ivd is defined as:

$$h(r_k) = n_k \quad for \quad k = 0, 1, 2, ...L-1 \tag{3}$$

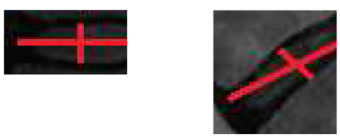

(a) IVD1 (b) IVD2

Fig. 7 Major and minor axis for two IVDs

where r_k for $k = 0, 1, 2, ...L-1$ denotes the intensities of L-level digital image ivd, n_k is number of pixels in ivd with intensity r_k.

3.2.2 Invariant moments

In object recognition, moments have been widely adopted for its invariant features [28]. The 2D $(p+q)^{th}$ order moment of an image $f(x, y)$, with size $M \times N$, is defined as [26]:

$$m_{pq} = \sum_{x=0}^{M-1} \sum_{y=0}^{N-1} x^p y^q f(x, y) \tag{4}$$

where $p = 0, 1, 2, ...$ and $q = 0, 1, 2, ...$

The central moments for the order $(p+q)$ are given by:

$$\mu_{pq} = \sum_{x=0}^{M-1} \sum_{y=0}^{N-1} (x - \overline{x})^p (y - \overline{y})^q f(x, y) \tag{5}$$

for $p = 0, 1, 2, ..., q = 0, 1, 2, ...,$ where,

$$\overline{x} = \frac{m_{10}}{m_{00}} \quad and \quad \overline{y} = \frac{m_{01}}{m_{00}} \tag{6}$$

The normalized central moment of order $(p+q)$, denoted by η_{pq}, is defined as:

$$\eta_{pq} = \frac{\mu_{pq}}{\mu_{00}^{\gamma}} \tag{7}$$

where,

$$\gamma = \frac{p+q}{2} + 1 \tag{8}$$

for $p + q = 2, 3, ...$

A set of moment invariants consists of nonlinear combinations of central moments that are rotation invariant. Hu [29] defined a set of seven 2D moment invariants which are derived from 2^{nd} and 3^{rd} central moments. These moments are invariant to object rotation, scale and translation. The IVDs are slightly rotated and vary in size. Hence, the moments are selected as another feature. The seven invariant moments [29] are defined as:

$$\phi_1 = \eta_{20} + \eta_{02} \tag{9}$$

$$\phi_2 = (\eta_{20} - \eta_{02})^2 + 4\eta_{11}^2 \tag{10}$$

$$\phi_3 = (\eta_{30} - 3\eta_{12})^2 + (3\eta_{21} - \eta_{03})^2 \tag{11}$$

$$\phi_4 = (\eta_{30} + \eta_{12})^2 + (\eta_{21} + \eta_{03})^2 \tag{12}$$

$$\phi_5 = (\eta_{30} - 3\eta_{12})(\eta_{30} + \eta_{12})\left[(\eta_{30} + \eta_{12})^2 - 3(\eta_{21} + \eta_{03})^2\right] + (3\eta_{21} - \eta_{03})(\eta_{21} + \eta_{03})\left[3(\eta_{30} + \eta_{12})^2 - (\eta_{21} + \eta_{03})^2\right] \tag{13}$$

$$\phi_6 = (\eta_{20} - \eta_{02})\left[(\eta_{30} + \eta_{12})^2 - (\eta_{21} + \eta_{03})^2\right] + 4\eta_{11}(\eta_{30} + \eta_{12})(\eta_{21} + \eta_{03}) \tag{14}$$

$$\phi_7 = (3\eta_{21} - \eta_{03})(\eta_{30} + \eta_{12})\left[(\eta_{30} + \eta_{12})^2 - 3(\eta_{21} + \eta_{03})^2\right] + (3\eta_{12} - \eta_{30})(\eta_{21} + \eta_{03})\left[3(\eta_{30} + \eta_{12})^2 - (\eta_{21} + \eta_{03})^2\right] \tag{15}$$

3.2.3 Gabor features

The texture of IVD differs with degenerative and non-degenerative discs. Also, the IVDs vary in size and orientation. The advantage of Gabor filter is invariant to rotation, scaling and translation [30]. Hence, Gabor features are also required to analyze the degenerative discs. The Gabor features that are based on Gabor filters were obtained from the grayscale images. A 2D Gabor filter in a spatial domain is a Gaussian kernel function modulated by a sinusoidal plane wave and defined as [30]:

$$g(x, y) = \exp\left(-\frac{x'^2 + \gamma y'^2}{2\sigma^2}\right)\exp\left(i\left(2\pi\frac{x'}{\lambda} + \psi\right)\right) \tag{16}$$

where

$$x' = x\cos\theta + y\sin\theta, \quad y' = -x\sin\theta + y\cos\theta, \tag{17}$$

λ is the wavelength of sinusoidal factor, θ represents the orientation of normal to parallel stripes of a Gabor function, ψ is the phase offset of sinusoidal function, σ is the standard deviation of Gaussian envelope and γ is the spatial aspect ratio and specifies ellipticity of support of Gabor function. In this paper, different wavelengths used are 2,4,6, 8 and 10, and orientations considered are 0, 15, 30, 45, 90, 120, 150 and 180. The phase offset is set as 0. The spatial aspect ratio is set as 0.25, and the standard deviation is set as 10. The sample Gabor filters for orientation = 0, 15 and wavelength = 2, 4 and its responses for a sample image are shown in Fig 8.

3.3 Classification

The obtained intensity, moments and Gabor features are linearly merged to form a feature vector F. In this work, training, testing and validation of the proposed model are based on SVM classifier. The SVM classifier aims to estimate a function $f : R^N \rightarrow \{\pm 1\}$ using the training data $D = (x_1, y_1), (x_2, y_2)...(x_l, y_l) \in R^N \times \pm\{1\}$, where x_i is N-dimensional real numbers R, y_i is class label. SVM will correctly classify a new data (x, y), i.e. $f(x) = y$, provided the data (x, y) are also collected from same underlying function as training data [31]. SVM classifier uses a hyperplane to separate the data points into classes. The hyperplane is defined as:

$$(w.x) + b = 0 \tag{18}$$

where w, b are weight and bias. The decision function is represented as:

$$f(x) = sign((w.x) + b) \tag{19}$$

SVM classification is based on the hyperplane and its corresponding decision functions. SVM is effective in high dimensional feature spaces [32]. The IVDs are needed to be classified as degenerative or non-degenerative disc. Hence, a binary class classification model is build using SVM to diagnose the degenerative disc in a mid-sagittal MR image.

3.3.1 Training and testing

The mid-sagittal lumbar MR images for 93 patients are used. Out of these images, 70% and 30% are selected for training and testing, respectively. In the training phase, training images are first segmented using EM-based IVD segmentation. Next, lumbar IVDs are cropped from the original mid-sagittal MR image. The cropped IVDs are categorized carefully as degenerative (ivd_D) and non-degenerative discs (ivd_{ND}). Now, the features such as basic intensity, invariant moments and Gabor features are extracted to form a hybrid feature vector F. The degenerative disc (ivd_D) is assigned

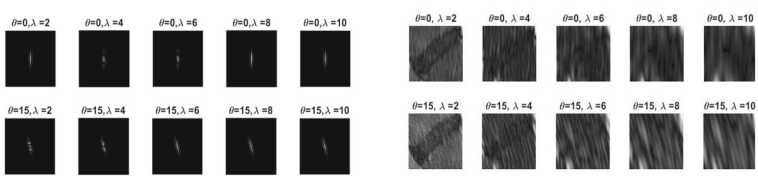

(a) Gabor filters (b) Magnitude responses

Fig. 8 Gabor filters and its magnitude responses

as class label $+1$ and non-degenerative discs (ivd_{ND}) as -1. A diagnostic model M is built using SVM classifier.

In the testing phase, a test image T is given as input, as shown in Fig 2. The test image T is a mid-sagittal MR image. Similar to the training phase, T is segmented to obtain lumbar IVDs (ivd). The features are obtained for the cropped six lumbar IVDs and given as input to model M. This model classifies the segmented lumbar discs as degenerative or non-degenerative discs and labels them as $+1$ or -1 accordingly.

3.3.2 Performance metrics

The EM-based new IVD segmentation method is validated using Dice Similarity Coefficient (DSC) and Intersection over Union (IoU) [33]. The system developed is tested and validated based on the performance metrics such as accuracy, sensitivity and specificity [34]. The accuracy is the measure of all correctly classified degenerative discs, sensitivity is the rate of degenerated discs that are correctly classified, and specificity is the rate of normal discs that are classified correctly.

4 Experimental results and discussion

4.1 Clinical Dataset

The dataset contains clinical lumbar MR images for 93 subjects. The images were collected from Metro scans, Thiruvananthapuram, India. The images were acquired by GE Signa 1.5 HDxt E MRI scanner, using a Fast Relaxation Fast Spin Echo (frFSE) imaging sequence. The acquisition parameters for T2-weighted sagittal images are: slice thickness = 4.5 mm, slice spacing = 0.6 mm. The resolution for all images is $512 \times 512 \times 3$. The degenerative disc diagnostic system is built from the clinical dataset. The segmentation is performed for all 93 images.

In order to construct a diagnostic model from the segmented images, the six lumbar IVDs are selected. Totally, there are 558 lumbar IVDs from all mid-sagittal lumbar MR images. Out of these 558 images, 221 IVDs are degenerative and 337 non-degenerative discs. The separated discs are analyzed for inter-rater reliability. Cohen's kappa (κ) coefficient is a statistical measure to determine the reliability between two raters. In this work, the separated images are analyzed by a radiologist (rater 1) and an orthopaedist (rater 2). Table 2 represents inter-observer variations. The κ coefficient derived from Table 2 is 0.92. This separation is ideal as it satisfies the condition ($0.8 \leq \kappa \leq 1$) [35].

4.2 Performance of IVD segmentation method

The degenerative disc diagnostic system is built from the clinical dataset. The segmentation is performed for all 93 images. The results for the proposed EM-based new IVD segmentation are calculated based on DSC and IoU. The DSC and IoU are calculated for each segmented image and its ground truth, and then, the average is found. The performance of IVD segmentation is presented in Table 3. DSC and IoU value ranges between 0 and 1. The value 0 means, there is no overlapping region between ground truth and segmented image. The value 1 means, segmented region and ground truth overlap perfectly. Also, the EM-based new IVD segmentation is compared with the segmentation performed by Ebrahimzadeh et al. [11]. The EM-based IVD segmentation method performs better than the state-of-the-art method, because the existing approach could not segment the IVDs properly if the IVD has an abnormality. The IVD segmentation is also compared with a deep learning architecture U-Net [36] and obtained an accuracy of 92.8%.

4.3 Performance of IVD classification

The performance of the proposed model is evaluated by conducting various experiments. First, the feature vector F is obtained. The features are derived from the gray scale image. The size of basic intensity feature is 6. The images are 8-bit graylevel; hence, the intensity histogram has 256 features. The number of features from invariant moments is 7. The number of Gabor features is 3000. Therefore, the length of this feature vector F is 3269.

Table 3 Performance of IVD segmentation method

Method	DSC	IoU
Threshold and Morphology based segmentation [11]	0.860	0.761
IVD Segmentation (Proposed)	0.883	0.801

Table 2 Inter-observer variations for degenerative disc diagnosis

		Rater 1	
		Non Degenerative Disc	Degenerative Disc
Rater 2	Non Degenerative Disc	328	9
	Degenerative Disc	11	210

The optimized hyper-parameters for SVM are estimated. The parameters obtained are $kernel = rbf$, $C = 0.259$ and $\gamma = 0.0227$. The 10-fold cross-validation is used to validate the proposed model. The main benefit of this method is that all data are used for both training and testing. The total number of training and testing images in each fold is presented in Table 4.

The hybrid of intensity, moments and Gabor features are extracted from the IVDs, and 10-fold cross-validation is performed. The average validation results with different classification model are presented in Table 5. The result shows the hybrid features with SVM classifier classifies the degenerative and non-degenerative discs in a better way, rather than other features and classifiers. The proposed model produces accuracy, sensitivity and specificity as 92.47%, 90.45% and 93.8%, respectively. The high sensitivity rate shows that the proposed system produces a low false negative rate, i.e. the proposed model diagnose the majority of all degenerative discs as degeneration correctly even if there is a minor abnormality.

In k-NN, the data itself are a model which is used for predictions and hence, training duration is reduced. However, k-NN does not perform well with a large dataset and high dimensionality. Even though training time is less, as there are more features in this proposed method, k-NN gives very low results. Decision trees are simple to understand and do not require normalized data for processing. However, overfitting is the major disadvantage of decision tree. LDA gives a better result when the data are linearly separable. If the data are not linearly separable, it tries to map in another space to maximum possible linear separable. In this method, as LDA could not separate the data linearly, comparatively it shows less performance than SVM. SVM is not suitable for large dataset. Despite this, SVM acts better in high dimensional space. Therefore, SVM achieves an improved result than other classifiers.

4.3.1 Patient-based performance analysis

The performance measure in the diagnosis of degenerative disc disease is evaluated per patient basis. In a total of 93 mid-sagittal clinical MR images, 70% (65 images) images are chosen for training and the remaining 30% (28 images) are chosen for testing. In the training phase, SVM model M is built using 70% images. In the testing phase, various performance metrics are evaluated for each patient based on the test result. The patient-based performance analysis is shown in Fig 9.

This performance evaluation shows that the proposed model produces an average accuracy, sensitivity and specificity of 92.86%, 90.87% and 95.21%, respectively. This proposed model diagnoses most of the degenerative discs but fails to diagnose a few of them. Overall, this system produces high sensitivity because the system is capable of diagnosing almost all degeneration in the image.

The output of this degenerative disc disease diagnosis system for 4 images is presented in Fig 10. In this figure, image 1 contains only one degenerative disc and it is diagnosed correctly. Similarly, in image 2 all lumbar IVDs are degenerative, and they are also diagnosed correctly. In image 3, there is no degenerative disc, and this system diagnoses it as no degeneration. In image 4, four discs are degenerative, but the system only diagnoses 3 discs as degenerative disc. The disc that missed out is collapsed disc. The proposed method could not diagnose such discs, because the height of disc is very less and the width is more than other discs. The intensity, moments and Gabor features are not sufficient to diagnose those discs.

4.3.2 Comparison with state-of-the-art technique

Moreover, this method is compared with the existing state-of-the-art methods in diagnosing degenerative discs. The comparison with the existing technique is performed on the private dataset discussed in Section 4.1. The degenerative disc diagnosis system has attained high accuracy, sensitivity and specificity when compared to the existing systems, and the results are shown in Table 6. The existing system could not diagnose degenerative discs, if the height of degenerative disc is similar to that of normal disc [16]. The proposed system eliminates this limitation.

5 Conclusion

The degenerative disc diagnosis system from the mid-sagittal lumbar MR image is proposed in this paper. An EM-based new IVD segmentation method is proposed to segment the IVDs from sagittal images. The segmented lumbar images contain a few thoracic, and lumbar IVDs. The lumbar IVDs are selected for further processing. This segmentation, segments all lumbar IVDs, even though it has abnormalities. The basic intensity, moments and Gabor features are extracted from the IVDs. Then, a classification model is built using SVM. The obtained features are classified as degenerative or non-degenerative discs by SVM classifier. The model is tested and validated using 10-fold cross-validation and produces an accuracy of 92.47%. The model is also evaluated for patient-based analysis and gives an accuracy of 92.86%. When compared with the state-of-the-art methods, the proposed method outperforms in terms of accuracy, sensitivity and specificity. This automated system has achieved high accuracy, sensitivity and specificity. Moreover, this system identifies minor abnormalities present in the disc. Hence,

Table 4 Number of IVDs used for training and testing in each fold

Fold	1	2	3	4	5	6	7	8	9	10
Training images	502	503	502	502	502	501	503	502	503	502
Testing images	56	55	56	56	56	57	55	56	55	56

Table 5 Classification results for 10-fold cross-validation

Classifier	Validation methods	Intensity	Histogram	Moments	Gabor features	Hybrid features
SVM	Accuracy(%)	68.47	72.62	70.27	87.28	92.47
	Sensitivity(%)	36.68	62.94	33.95	83.7	90.45
	Specificity(%)	89.29	78.94	94.1	89.63	93.8
k-NN	Accuracy(%)	67.78	82.62	62.01	80.12	83.69
	Sensitivity(%)	50.22	68.81	42.92	82.79	73.15
	Specificity(%)	79.3	91.72	74.45	78.37	90.54
Decision Tree	Accuracy (%)	63.44	79.22	63.26	83.18	76.14
	Sensitivity(%)	51.94	72.81	40.69	79.15	73.35
	Specificity(%)	70.93	83.39	78.04	85.8	78.04
LDA	Accuracy (%)	67.94	67.03	70.26	80.64	78.51
	Sensitivity(%)	36.68	36.28	33.93	83.24	73.72
	Specificity(%)	88.45	87.19	94.06	78.93	81.61
Feedforward Neural Network	Accuracy (%)	66.47	80.84	71.43	80.24	83.23
	Sensitivity(%)	25.76	68.18	59.09	72.27	80.30
	Specificity(%)	93.07	89.11	79.41	82.18	85.15

Fig. 9 Patient-based analysis

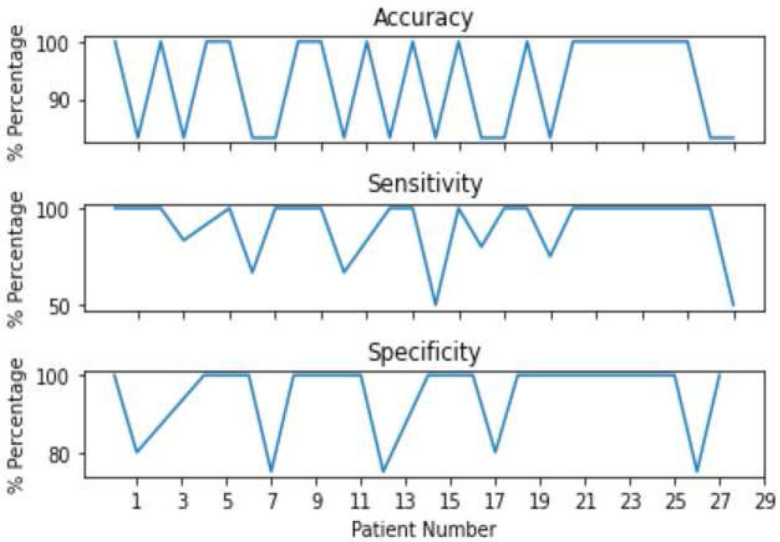

Fig. 10 Degeneration diagnosis for Image 1, Image 2, Image 3 and Image 4

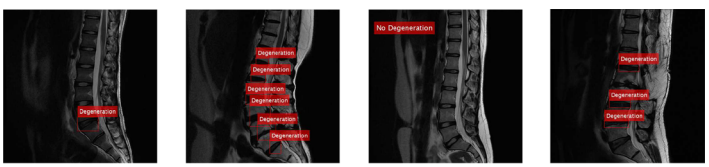

(a) Image 1 (b) Image 2 (c) Image 3 (d) Image 4

Table 6 Comparison with state-of-the-art methods

Method	Accuracy (%)	Sensitivity (%)	Specificity (%)
ML based method [13]	76.52	69.22	81.27
Euclidean distance method [16]	82.44	89.42	73.57
Disc degeneration diagnosis system (proposed)	92.47	90.45	93.8

this system can be used as a second opinion in diagnosing degenerative discs.

Declarations

Conflict of Interest The authors declare that they have no conflict of interest.

References

1. Hartvigsen, J., Hancock, MJ., Kongsted, A., Louw, Q., Ferreira, ML., Genevay, S., Hoy, D., Karppinen, J., Pransky, G., Sieper, J.: et al. What low back pain is and why we need to pay attention
2. Hurwitz, Eric L., Randhawa, Kristi, Yu, Hainan, Côté, Pierre, Haldeman, Scott: The global spine care initiative: a summary of the global burden of low back and neck pain studies. Eur. Spine J. **27**(6), 796–801 (2018)
3. Trompeter, K., Fett, D., Brüggemann, G-P., Platen, P.: Prevalence of back pain in elite athletes. *German Journal of Sports Medicine/Deutsche Zeitschrift fur Sportmedizin*, 69, (2018)
4. Richard Bowyer R.O. Bigos, S.J., Richard Braen, G.:(1996) Acute low back problems in adults, ahcpr guideline no 14 *Journal of Manual & Manipulative Therapy*, 4(3):99–111,
5. Chou, Roger, Qaseem, Amir, Snow, Vincenza, Casey, Donald, Cross, J Thomas, Shekelle, Paul, Owens, Douglas K.: Diagnosis and treatment of low back pain: a joint clinical practice guideline from the american college of physicians and the american pain society. Ann. Int. Med. **147**(7), 478–491 (2007)
6. Zaidi, H., Del Guerra, A.: An outlook on future design of hybrid pet/mri systems. Med. Phys. **38**(10), 5667–5689 (2011)
7. Hasz, Michael W.: Diagnostic testing for degenerative disc disease. *Advances in orthopedics*, 2012, (2012)
8. Tertti, Minna, Paajanen, Hannu, Laato, Matti, Aho, HEIKKI, Komu, Makku, Kormano, Martti.: (1991) Disc degeneration in magnetic resonance imaging. a comparative biochemical, histologic, and radiologic study in cadaver spines. *Spine*, 16(6):629–634
9. Doi, Kunio: Computer-aided diagnosis in medical imaging: historical review, current status and future potential. Comput. Med. Imag. Graph. **31**(4–5), 198–211 (2007)
10. Ayed, Ismail Ben, Punithakumar, Kumaradevan, Garvin, Gregory, Romano, Walter, Li, Shuo.: Graph cuts with invariant object-interaction priors: application to intervertebral disc segmentation. In *Biennial International Conference on Information Processing in Medical Imaging*, pages 221–232. Springer, 2011
11. Ebrahimzadeh, Elias, Fayaz, Farahnaz, Ahmadi, Fereshte, Nikravan, Mehran: A machine learning-based method in order to diagnose lumbar disc herniation disease by mr image processing. MedLife Open Access **1**(1), 1 (2018)
12. Beulah, A., Sree Sharmila, T.: Classification of intervertebral disc on lumbar mr images using svm. In *2016 2nd International Conference on Applied and Theoretical Computing and Communication Technology (iCATccT)*, pages 293–297. IEEE, 2016
13. Oktay, Ayse Betul, Albayrak, Nur Banu, Akgul, Yusuf Sinan .: Computer aided diagnosis of degenerative intervertebral disc diseases from lumbar mr images. *Computerized medical imaging and graphics*, 38(7):613–619, 2014
14. Beulah, A., Sharmila, T Sree., Pramod, VK.:(2018) Disc bulge diagnostic model in axial lumbar mr images using intervertebral disc descriptor (idd). *Multimedia Tools and Applications*, 77(20): 27215–2723
15. Beulah, A., Sharmila, T Sree., Kanmani, T.: Spinal cord segmentation in lumbar mr images. In *International Conference on Emerging Current Trends in Computing and Expert Technology*, pages 1226–1236. Springer, (2019)
16. Mahdy, Lamia Nabil., Ezzat, Kadry Ali., Hassanien, Aboul Ella.: Automatic detection system for degenerative disk and simulation for artificial disc replacement surgery in the spine. *ISA transactions*, 81:244–258, (2018)
17. Raja'S, Alomari, Corso, Jason J., Chaudhary, Vipin, Dhillon, Gurmeet.: Desiccation diagnosis in lumbar discs from clinical mri with a probabilistic model. In *2009 IEEE International Symposium on Biomedical Imaging: From Nano to Macro*, pages 546–549. IEEE, 2009
18. da Silva Barreiro, Marcelo, Nogueira-Barbosa, Marcello H., Rangayyan, Rangaraj M., de Menezes Reis, Rafael, Pereyra, Lucas Calabrez, Azevedo-Marques, Paulo M.: Semiautomatic classification of intervertebral disc degeneration in magnetic resonance images of the spine. In *5th ISSNIP-IEEE Biosignals and Biorobotics Conference (2014): Biosignals and Robotics for Better and Safer Living (BRC)*, pages 1–5. IEEE, 2014
19. Unal, Y., Kocer, HE., Akkurt, HE.: A comparison of feature extraction techniques for diagnosis of lumbar intervertebral degenerative disc disease. In *2011 International Symposium on Innovations in Intelligent Systems and Applications*, pages 490–494. IEEE, (2011)
20. Unal, Y., Kocer, HE., Akkurt, HE.: Automatic diagnosis of intervertebral degenerative disk disease using artificial neural network. In *6th International Advanced Technologies Symposium (IATS–11)*, pages 16–18, (2011)
21. Neubert, A., Fripp, J., Engstrom, C., Walker, D., Weber, M.A., Schwarz, R., Crozier, S.: Three-dimensional morphological and signal intensity features for detection of intervertebral disc degeneration from magnetic resonance images. J. Am. Med.l Inform. Associat. **20**(6), 1082–1090 (2013)
22. Castro-Mateos, Isaac, Hua, Rui, Pozo, Jose M., Lazary, Aron, Frangi, Alejandro F.: Intervertebral disc classification by its degree of degeneration from t2-weighted magnetic resonance images. Eur. Spine J. **25**(9), 2721–2727 (2016)
23. Unal, Yavuz, Polat, Kemal, Kocer, H Erdinc, Hariharan, M.: Detection of abnormalities in lumbar discs from clinical lumbar mri with hybrid models. Appl. Soft Comput. **33**, 65–76 (2015)
24. Dempster, Arthur P., Laird, Nan M., Rubin, Donald B.: Maximum likelihood from incomplete data via the em algorithm. Journal of the Royal Statistical Society: Series B (Methodological) **39**(1), 1–22 (1977)

25. Dougherty, Edward R.: *Digital image processing methods*. Marcel Dekker, Inc., (1994)
26. Gonzalez, Rafael C., Wintz, Paul.: Digital image processing(book). *Reading, Mass., Addison-Wesley Publishing Co., Inc.(Applied Mathematics and Computation*, (13):451, (1977)
27. Chow, Daniel HK., Yuen, Ernest MK., Xiao, L., Leung, Mason CP.: Mechanical effects of traction on lumbar intervertebral discs: a magnetic resonance imaging study. Musculoskeletal Science and Practice **29**, 78–83 (2017)
28. Mercimek, Muharrem, Gulez, Kayhan, Mumcu, Tarik Veli: Real object recognition using moment invariants. sadhana **30**(6), 765–775 (2005)
29. Ming-Kuei, Hu.: Visual pattern recognition by moment invariants. IRE transactions on information theory **8**(2), 179–187 (1962)
30. Haralick, Robert M.: Statistical and structural approaches to texture. Proceedings of the IEEE **67**(5), 786–804 (1979)
31. Hearst, Marti A., Dumais, Susan T., Osuna, Edgar, Platt, John, Scholkopf, Bernhard: Support vector machines. IEEE Intell. Syst. Appl. **13**(4), 18–28 (1998)
32. Kim, Kwang In., Jung, Keechul, Park, Se Hyun, Kim, Hang Joon.: Support vector machines for texture classification. *IEEE transactions on pattern analysis and machine intelligence*, 24(11):1542–1550, 2002
33. Qin, Fangbo, Li, Yangming, Su, Yun-Hsuan, Xu, De, Hannaford, Blake.: Surgical instrument segmentation for endoscopic vision with data fusion of rediction and kinematic pose. In *2019 International Conference on Robotics and Automation (ICRA)*, pages 9821–9827. IEEE, 2019
34. Baratloo, Alireza, Hosseini, Mostafa, Negida, Ahmed, El Ashal, Gehad.: Part 1: simple definition and calculation of accuracy, sensitivity and specificity. (2015)
35. McHugh, Mary L.: Interrater reliability: the kappa statistic. Biochemia medica: Biochemia medica **22**(3), 276–282 (2012)
36. Ronneberger, Olaf, Fischer, Philipp, Brox, Thomas.: U-net: Convolutional networks for biomedical image segmentation. In *International Conference on Medical image computing and computer-assisted intervention*, pages 234–241. Springer, (2015)

A. Beulah is working as Assistant professor in Department of Computer Science and Engineering at SSN College of Engineering, Chennai. She received her Ph.D. from Anna University, Chennai in 2021. She received her M. Tech degree First class with distinction from National Institute of Technology, Thiruchirapalli in 2007. She also received her B.E degree First class with distinction from Sethu Institute of Technology, Madurai in 2002. She was Lecturer at University College of Engineering, Trivandrum until 2005. After completing her M.Tech she joined in the department of Computer Science and Engineering as Lecturer at SSN College of Engineering, India during 2007. Her primary research interests include Medical Image Processing and Analysis. She has published papers in international journals and conferences.

T. Sree Sharmila is working as Associate Professor in the Department of Information Technology, SSN College of Engineering, Chennai, India. She received her BE in Information Technology from Manonmaniam Sundaranar University, Tirunelveli, in 2003, ME in Computer Science and Engineering from Annamalai University, Chidambaram, in 2005 and PhD from Anna University, Chennai, in 2013. She has published more than 30 papers in well renowned International and National Journals and Conferences and has guided 9 research scholars. Her areas of interest are image preprocessing, texture analysis, satellite, medical and underwater image analysis.

V. K. Pramod is working as Assistant Professor, Orthopaedics at Government Medical College, Trivandrum. He received his bachelor degree in Medicine (MBBS) at Government Medical College, Trivandrum in 1999. He received his Master of surgery in orthopaedics from Government Medical college, Kottayam in 2004. He is specially interested in arthroscopic surgery of knee, shoulder and conservative management of discogenic low back pain. He has published papers in journals and conferences.